Eur Biophys J (2007) 37:19–33
DOI 10.1007/s00249-007-0149-z

ORIGINAL PAPER

Monte Carlo simulations of tBid association with the mitochondrial outer membrane

Valery G. Veresov · Alexander I. Davidovskii

Received: 18 October 2006 / Revised: 2 February 2007 / Accepted: 24 February 2007 / Published online: 21 March 2007

Abstract Bid, a BH3-only pro-apoptopic member of the BCL-2 protein family, regulates cell death at the level of mitochondrial cytochrome *c* efflux. Bid consists of 8 α-helices (H1–H8, respectively) and is soluble cytosolic protein in its native state. Proteolysis of the N-terminus (encompassing H1 and H2) of Bid by caspase 8 in apoptosis yields activated ''tBid'' (truncated Bid), which translocates to the mitochondria and induces the efflux of cytochrome c. The release of cytochrome c from mitochondria to the cytosol constitutes a critical control point in apoptosis that is regulated by interaction of tBid protein with mitochondrial membrane. tBid displays structural homology to channel-forming bacterial toxins, such as colicins or transmembrane domain of diphtheria toxin. By analogy, it has been hypothesized that tBid would unfold and insert into the lipid bilayer of the mitochondria outer membrane (MOM) upon membrane association. However, it has been shown recently that unlike colicins and the transmembrane domain of diphtheria toxin, tBid binds to the lipid bilayer maintaining α-helical conformation of its helices without adopting a transmembrane orientation by them. Here, the mechanism of the association of tBid with the model membrane mimicking the mitochondrial membrane is studied by Monte Carlo simulations, taking into account the underlying energetics. A novel two-stage hierarchical simulation protocol combining coarse-grained discretization of conformational space with subsequent refinements was applied which was able to generate the protein conformation and its location in the membrane using modest computational resources. The simulations show that starting from NMR-established conformation in the solution, the protein associates with the membrane without adopting the transmembrane orientation. The configuration (conformation and location) of tBid providing the lowest free energy for the system protein/membrane/solvent has been obtained. The simulations reveal that tBid upon association with the membrane undergoes significant conformational changes primarily due to rotations within the loops between helices H4 and H5, H6 and H7, H7 and H8. It is established that in the membrane-bound state of tBid-monomer helices H3 and H5 have the locations exposed to the solution, helices H6 and H8 are partly buried and helices H4 and H7 are buried into the membrane at shallow depth. The average orientation of tBid bound to the membrane in the most stable configuration reported here is in satisfactory agreement with the evaluations obtained by indirect experimental means.

Keywords Apoptosis · Bid · Mitochondria · Protein insertion · Cardiolipin

Introduction

Programmed cell death or apoptosis is a normal physiological form of cell death whereby the removal of infected, damaged, or unwanted cells occurs. This process plays a key role in the successful embryonic development and the maintenance of cellular homeostasis (Daniel and Korsmeyer 2004; Adams 2003). Two major apoptotic pathways, intrinsic and extrinsic, have been identified which are both

Electronic supplementary material The online version of this article (doi:10.1007/s00249-007-0149-z) contains supplementary material, which is available to authorized users.

V. G. Veresov (✉) · A. I. Davidovskii
Department of Cell Biophysics,
Institute of Biophysics and Cell Engineering,
Academicheskaya St. 27, Minsk 220072, Belarus
e-mail: veres@biobel.bas-net.by

regulated by pro-apoptopic as well as anti-apoptotic proteins of the BCL-2 protein family (Gross et al. 1999a, b; Cory et al. 2003). The cell-intrinsic apoptotic pathway involves activation of proapoptotic BCL-2 family members, which induce the permeabilization of the mitochondrial outer membrane (MOM), resulting in the release of cytochrome *c* (Cyt *c*) and other proteins from intermembrane space of mitochondria (Wang 2001). In the extrinsic pathway, apoptosis is initiated through activation of members of the tumor necrosis factor (TNF)/Fas receptor family (Varfolomeev and Ashkenazi 2004). Once engaged by ligand, these receptors initiate the formation of the death-inducing signaling complex (DISC), which leads to activation of caspase-8. Activated caspase-8 can initiate both a cascade of caspases and the cleavage of the BID protein.

BID is a pro-apoptotic member of the ''BH3-only'' subset of the BCL-2 family proteins (Wang et al. 1996; Willis and Adams 2005; Yin 2006) that interconnects extrinsic pathway TNFR1 and Fas death signals to the mitochondrial amplification of the intrinsic pathway. Bid was originally identified in a yeast two-hybrid screen as a protein that interacted with both Bcl-2 and Bax via their BH3 domains and induced apoptosis when it was overexpressed in cells (Wang et al. 1996). Bid is normally present in inactive form in the cytosol. In response to stimuli of the extrinsic, death receptor, pathway Bid is proteolytically cleaved by caspase 8 and thus activated (Li et al. 1998). The solution structure of Bid has been resolved using NMR-spectroscopy (Chou et al. 1999; McDonnel et al. 1999). Bid has 8 α-helices (designated H1 through 8) of which two central mostly hydrophobic helices (H6 and H7) are surrounded by six amphipatic helices. The cleavage of cytosolic 22-residues (p22) BID at Asp59 by activated caspase 8 within an unstructured loop yields an N-terminal 7-kDa fragment, which includes helices H1 and H2, and a C-terminal 15-kDa fragment, which includes helices H3 through H8 (Li et al. 1998; Luo et al. 1998; Gross et al. 1999a, b). Cleaved Bid, tBid (truncated Bid) lacks H1 and H2 and, as the result, the essentially hydrophobic hairpin structure formed by H6 and H7 becomes exposed. Cleaved BID then undergoes posttranslational modification by myristoylation at a newly generated N-terminal glycine of the p15-kDa fragment (p15 BID or tBID; Zha et al. 2000). Myristoylated tBID now translocates to mitochondria where it localizes to mitochondrial contact sites where cardiolipin has been reported to exist (Lutter et al. 2000; Kim et al. 2004). Targeted tBID cooperates with multidomain pro-apoptotic BAX in the MOM to permeabilize it (Wei et al. 2000; Eskes et al. 2000; Kuwana et al. 2002) that leads to a release of intermembrane space proteins, including cytochrome *c* which forms an apoptosome complex with Apaf-1 and caspase-9 to activate effector caspases (Korsmeyer et al. 2000; Opferman and Korsmeyer 2003; Adams 2003). In addition to the role of tBID in activation of the critical gateway proteins BAX and BAK, targeted p15 BID also triggers remodeling of the inner membrane and the cristae structure of the mitochondria in a BAX-, BAK-independent manner, resulting in the mobilization of the majority of cytochrome *c* within the cristae that is stored in the intermembrane space of the organelle (Scorrano et al. 2002).

The structural arrangement of α-helices within tBid is conserved among other Bcl-2 family proteins, such as Bcl-2, Bcl-X_L and Bax, and is also similar to that of the membrane translocation domains of bacterial toxins such as colicins and diphtheria toxins (Muchmore et al. 1996; Chou et al. 1999). These domains of bacterial toxins consist of α-helices in which two contiguous hydrophobic α-helices form a helical hairpin structure that is surrounded by other helices (Choe et al. 1992; Zakharov and Cramer 2002). The helical hairpin inserts into the membrane in a transmembrane orientation when the toxin molecules bind to the lipid bilayer (Cramer et al. 1995; Stroud et al. 1998; Zakharov and Cramer 2002; Rosconi et al. 2004). In BID, helices H6 and H7 correspond to the ''helical hairpin region'' of membrane-translocating bacterial toxins and a similar region proposed for BCL-XL (Muchmore et al. 1996; Chou et al. 1999), implying a role of Bid in pore formation. Several experimental studies provided seemingly support for the poration activity of tBid (Schendel et al. 1999; Kudla et al. 2000; Grinberg et al. 2002). In contrast, it has been reported recently elsewhere that tBid associates with the membranes of lipid bilayers with its helices near parallel to the membrane surface and without significant transbilayer insertion (Garcia-Saez et al. 2004; Gong et al. 2004; Oh et al. 2005; Mau et al. 2006).

Elucidation of the structural mechanism of tBid action requires knowledge of its three-dimensional structure in the membrane-bound state and the conformational changes it undergoes. Though the structural biology of the Bcl-2 family of proteins has developed significantly during the past decade (Petros et al. 2004), structural studies of their interactions with membranes are most challenging technically, and the main details have still not been resolved. The experimental analysis is seriously hampered by difficulties in the preparation of suitable samples containing proteins in the membrane-bound state. Because of this, X-ray crystallography and NMR spectroscopy, which have been enormously successful in revealing the structure of soluble proteins, face formidable difficulties when applied to membrane proteins. As a result, only a minor part of membrane protein structures are known at atomic resolution so far and the structure/function relationships of membrane proteins are not well understood. As for Bid, only the structure of the inactive, water-soluble form is known at present time (Chou et al. 1999; McDonnel et al.

1999). Most of our information about tBid/ mithochondrial membrane interactions stems from a variety of biochemical and biophysical (mainly spectroscopic and indirect) experiments that give only low-resolution, essentially macroscopic, structural information. Given these arguments, computer modeling could make a significant contribution and be a significant complement of experimental studies. The most detailed and accurate approach to modeling the protein interactions with the membrane involves explicit representation of the membrane lipid and water molecules used in molecular dynamics (MD) simulations (reviewed in Ash et al. 2004; Bond and Sansom 2004, 2006; Gumbart et al. 2005; Sperotto et al. 2006). All-atom explicit simulations provide the most realism but have a prohibitive cost in terms of computing time required for the analysis. In addition, they require laborious procedures to provide information on the thermodynamics of the insertion or folding process. Typically, the information that can be obtained by MD simulations is limited at 70-residues proteins and on a nanosecond time-scale. Moreover, even very long (by current standards, about 100 ns for the protein of ~100 residues) simulations of protein–membrane systems give results dependent on the initial conditions and is thus unable to predict optimal location and conformation of such proteins (peptides) with respect to membrane. A promising alternative approach lies in employment of Monte Carlo (MC) method (Metropolis et al. 1953) with an implicit representation of both the membrane and the solvent. Such an approach is significantly less computationally expensive than explicit solvent-protein-membrane consideration and, therefore, is able to address questions about structure and function of membrane proteins determined by processes on rather larger time scales. The MC method has been demonstrated to be an important tool in the investigation of protein-membrane interactions in many cases (Milik and Skolnick 1993, 1995; Sung 1994, 1995; Baumgaertner 1996; Sintes and Baumgaertner 1998; Ducarme et al. 1998; Efremov et al. 1999a, b, 2002; Maddox and Longo 2002; Kessel et al. 2003; Mungikar and Forciniti 2004; Tzlil and Ben-Schaul 2005).

Here, we report the results of the MC analysis of the interactions between tBid and the model lipid monolayer represented in such a way as to duplicate the structure of the MOM formed by anionic lipids. We determined the most probable configuration of tBid associated with the membrane which provides the lowest free energy for the system protein/membrane/solvent and addressed aspects related to permeabilization process of the MOM by concerted action of tBid and Bax. We showed that association of tBid with membrane formed by anionic lipids leads to significant conformational changes primarily within interhelical loops and to orientations of the helices H6–H8 near parallel to the membrane surface predominantly at the boundary region of the membrane slab between anionic surface of the membrane and its hydrophobic moiety formed by hydrocarbon chains.

Materials and methods

The membrane model

It is agreed that tBid binds to mitochondrial contact sites of the MOM (Lutter et al. 2000; Kim et al. 2004). The contact site region of the MOM is thought to be a lipid bilayer containing an asymmetrical distribution of lipids across the two leaflets, of which the inner one is formed by neutral lipids and the outer one is formed by a mixture of anionic lipids (cardiolipins) and neutral lipids (phosphatidylcholines and phosphatidylethanolamines; Ardail et al. 1990). The implicit membrane model for the MOM contact site region was used. With this model, the membrane was represented as a ''hydrophobic slab'' with the plane of smeared negative charge (corresponding to the position of the centers of cardiolipins headgroups) offset from the membrane surface (located at z_w) by 4 Å inward the membrane in accordance with the data on the thickness of headgroup region (Peitsch et al. 1995). The effective surface charge density σ was assumed to be a sum of negative surface charge density due to acidic lipids in the membrane and a positive surface charge density due to membrane-adsorbed cations.

The protein model

The total potential energy function for protein was taken in the form:

$$U = U_{\mathrm{ECEPP}/2/3} + U_{\mathrm{S}} + U_{\mathrm{el,m}}. \quad (1)$$

The term $U_{\mathrm{ECEPP/2/3}}$ includes ECEPP2/ ECEPP3 van der Waals, torsion, electrostatic and hydrogen contributions (Dunfield et al. 1978; Némethy et al. 1983, 1992). The hydrophaties of the amino acid side chains and the hydrophilicities of the polypeptide backbone were taken into account by the term U_s by introducing the corresponding energy (U_s) of transfer of the protein from a polar aqueous environment to the hydrophobic core of the membrane

$$U_S = \sum_{j=1}^{N} (s_j ASA_{s,j} + c_j ASA_{b,j}) g(z_j), \quad (2)$$

where s_j and c_j are the average energy of transport of a side-chain group and a peptide group, respectively; $\mathrm{ASA}_{s,j}$ and $\mathrm{ASA}_{b,j}$ are accessible surface areas of side chain C_β-atom and backbone O-atom, respectively. The function $g(z_i)$ was

taken in accordance with the corresponding function of Baumgaertner (1996). The Roseman hydrophobicity scale (Roseman 1988) have been used to determine s_j. ASAs were determined by the program GETAREA (Fraczkiewich and Braun 1998). The parameter c_j represents the hydrophilicity of the peptide group and takes into account the loss of hydrogen bond energy of a backbone group with water during the insertion into the hydrophobic region of the membrane. Just as in the work of Baumgaertner (1996), the latter energy contribution was assumed to be independent of j, and was taken $c_j = c = 4$ kcal/mol. Because in the present study water molecules are not explicitly taken into account, one must introduce an interfacial profile function that describes the change of fraction of water with distance $z_j - z_W$ from the interfacial membrane plane located at z_W. Just as in the works of Baumgaertner and Efremov et al. (Baumgaertner 1996; Efremov et al. 1999), this profile function was assumed to vary exponentially with the distance from membrane interface:

$$g(z_j) = \frac{1}{1 + \exp[(z_j - z_w)/\lambda]}, \tag{3}$$

where the decay length λ was taken equal to –2 Å (the minus sign was used to account for the water phase disposition to the right of the membrane).

The influence of the layer of negatively charged headgroups of cardiolipins is taken into account by introducing the term $U_{m,el}$ for the electrostatic interaction energy of the protein

$$U_{m,el} = F\sum_i q_i \varphi(z_i) \tag{4}$$

where q_i and z_i are the partial charge and coordinate z of atom i, and F is Faraday's constant.

Two types of potential ϕ(z) were used. The Gouy–Chapman potential for the electrical double layer (McLaughlin 1989; Lazaridis 2005) was applied outside the membrane slab:

$$\varphi(z) = \frac{2RT}{zF} \ln \frac{[1 + \alpha_1 \exp(-\kappa(z - z_w)]}{[1 - \alpha_1 \exp(-\kappa(z - z_w)]}, \tag{5}$$

where $\alpha_1 = \frac{\exp(F\varphi_0/2RT)-1}{\exp(F\varphi_0/2RT)+1}$, φ_0 is the surface potential, which for a symmetric electrolyte is given by

$$\sinh\left[\frac{z_v F \varphi_0}{2RT}\right] = \frac{\sigma}{\sqrt{8\varepsilon_r \varepsilon_0 \rho RT}}. \tag{6}$$

Here, z_v is the valence of electrolyte, e is the charge of a proton, σ is the effective surface charge density, ε_0 is the permittivity of vacuum and ε_r is the relative permittivity, and κ is the inverse Debye length:

$$\kappa = \sqrt{\frac{2\rho z_v^2 F^2}{\varepsilon_r \varepsilon_0 RT}}. \tag{7}$$

(Although the derivation of the expression (6) rests on the assumption of the zero normal component of field strength at the charge plane on its hydrophobic inside resulting in the independence of two surface potentials (Nelson et al. 1975) that is not rigorously correct in general case, the use of (6) can be justified based on the results of the numerical integration of the Poisson–Boltzmann nonlinear equation for membrane–electrolyte systems (Nelson et al. 1975; Forsten et al. 1994) as well as analytical estimates (Winterhalter and Helfrich 1992) showing that the error caused by the use of Eq. 6 is small in the case when $(\varepsilon_m/\varepsilon_a)(1/\kappa d) \ll 1$, where ε_m, ε_a are dielectric permittivities of the membrane lipid phase and of the solution, respectively, κ is the inverse Debye screening length and d is the membrane width).

The estimate of σ was made by the use of the expression (8)

$$\sigma = \frac{e_0(z_N X_N + \sum_i z_i X_i)}{S(1 + PX_N - X_N)}, \tag{8}$$

where e_0 is the proton charge, S is the surface area per neutral lipid [assumed to be 68 Å^2 (Peitsch et al. 1995)], P is the ratio of the surface areas of negative to neutral lipid [assumed to be 2 for mitochondrial contact site cardiolipin-phosphatidylcholine-phosphatidylethanolamine lipid composition (Schlame et al. 2000)], X_N is the mole fraction of negatively charged lipids [assumed to be 27% (Ardail et al. 1990)], z_N is the signed charge of the cardiolipin headgroup, X_i is the mole fraction of bound cation i per mole of total lipid, and z_i is the valence of cation. The calculation of the adsorption of positive charge to the surface of the membrane was realized using the Gouy–Chapman–Stern equation and Langmuir adsorption isotherm (McLaughlin 1989) with association constant $K = 0.3\ M^{-1}$. As a result, the value of σ equal to e/(271 Å^2) was obtained to be used in the simulations.

For simplicity, the expression (5) was approximated during simulations by the expression

$$\varphi(z) = \mu(z)\exp(-\kappa(z - z_w)), \tag{9}$$

where the function μ(z) was taken as

$$\mu(z) = \frac{\varphi_0 + B_L(z - z_w)}{1 + (z - z_w)}; \quad B_L = \frac{4RT\alpha_1}{zF} \tag{10}$$

The expressions (9) and (10) are mathematically obvious if to take into account that Taylor's expansion of (5) on y, where $y = \exp(-\kappa(z - z_w))$ gives, when $(z - z_w) \gg 1$,

$\varphi(z) \approx B_L y = B_L \exp(-\kappa(z - z_w))$ and that when $z - z_w \approx 0, \mu(z) \approx \varphi_0$, thus, the expression (9) approximates satisfactory (5) both at small and great distances from the membrane. Although Eqs. 5 and 6 of the Gouy–Chapman theory are derived under the assumption of constant dielectric permittivity, the distance-dependent values of the dielectric permittivity were applied when using (9) in order to mimic more adequately the electrostatic potential profile in the vicinity of the membrane. The continuous dielectric profile was used with $\varepsilon_r = 4(z - z_w + 6$ Å) in the aqueous and lipid phases when –5 Å $< (z - z_w) < 14$ Å, $\varepsilon_r = 4$ in the lipid phase for $|z - z_w| > 5$ Å and $\varepsilon_r = 80$ in the aqueous phase, when $(z - z_w) > 14$ Å. Mathematically, the expression (9) with the dielectric permittivity varying with distance can be considered as joining the asymptotical expansions of two solutions of Poisson–Boltzmann equations (5) obtained each under the assumption of constant dielectric permittivities corresponding to the regions of small and great distance from the membrane surface. In the case of 0.1 M monovalent electrolyte, the dielectric profile taken leads to values of $\kappa \approx 1/(10$ Å) when $(z - z_w) > 14$ Å and to value of $\kappa \approx 1/(3.9$ Å) at $z = z_W$. The ''constant field'' approximation was used within the hydrophobic core of the membrane leading to the linear increase of potential with the increase of distance from the charged surface. The potential at the membrane–solution interface of the inner monolayer of MOM formed by neutral lipids was set equal to zero in accordance with the arguments above assuming that two surface potentials on both sides of the membrane are independent of each other as well as in accordance with the assumptions of the absence of the MOM resting potential (Benz et al. 1990). To approximate the electrostatic potential distribution within the headgroup region outside the Van der Waals envelopes of the polar headgroups, the constant potential was used between $z_{mc} - 2$ Å and $z_{mc} + 2$ Å, where z_{mc} is the z-coordinate of the plane containing the centers of charged headgroups (Ohshima and Kondo 1988). The field strength in the interval between the membrane surface at z_w and $z_{mc} + 2$ Å was taken to be constant and was set equal to that at the membrane surface. The potential profile constructed in accordance with the model assumptions and Eqs. 9 and 10 is shown in Fig. 1.

Simulation protocol

Two-stage hierarchical simulation protocol was used. At the first coarse-grained stage, a method combining Metropolis Monte Carlo search (Metropolis et al. 1953) on the space of configurations of tBid relative to the membrane with preliminary selective coarse-grained discretization and fixing of backbone conformational space and with simplifying consideration of side chains was applied. At the second stage, several low-energy structures obtained at the first stage were refined by using Monte Carlo conformational-configurational search on complete space of generalized coordinates describing the conformation of the protein and its localization relative to the membrane.

Coordinates of the tBid starting structures atoms were taken from Protein Data Bank entry 1ddb (McDonnel et al. 1999). It is clear that a straightforward sampling of conformational space during the consideration of the protein insertion into the membrane is computationally ineffective, because we have to search a high-dimensional conformational space rather than discrete space. Conventional Metropolis Monte Carlo method samples the whole space by making small increments in each step. The large energy barriers in the conformational space of the protein make such a method impractical because, for most of the time, the sampling is confined to a very restricted region of the whole conformational space. To overcome these difficulties, several approaches have been developed (Kirkpatrick et al. 1983; Li and Scheraga 1987; Chang et al. 1989; Lee et al. 1997; Pillardy et al. 2000, 2001; Ozkan and Meirovitch 2004; Zhan et al. 2006). One of the most popular methods is the Monte Carlo-minimization (MCM) method (Li and Scheraga 1987). With MCM, at each step a conformational change of the current structure is carried out by selecting at random a small number of dihedral angles, defining their new values at random, and minimizing the energy of the obtained structure; the obtained trial structure is accepted in accordance with Metropolis criteria. Though MCM allows one to reduce significantly the number of calculations on the way to global minimum, the method still contains computationally expensive elements such as frequent repeated returnings of the system to the earlier visited energy basins during simulations. To overcome this problem, we have decided for crude analysis of protein insertion into the membrane instead of Monte Carlo steps followed by the minimization, which is typical for MCM, to reverse these procedures and to realize the minimizations prior to Monte Carlo runs. On our opinion, such an approach, named minimization-Monte Carlo (MMC), should increase the efficiency of the search for global minimum of the membrane–protein system. Our hierarchical approach included two stages.

Stage (i)

This stage was realized by the MMC approach. At this stage, based on experimental data and simple hydrophobic analysis, a number of regions [named, simulation domains (SDMs)] within tBid were suggested to be inserted into the membrane without the significant conformational changes of their backbones and as such, for coarse-grained analysis, most of the backbone dihedral angles determining the

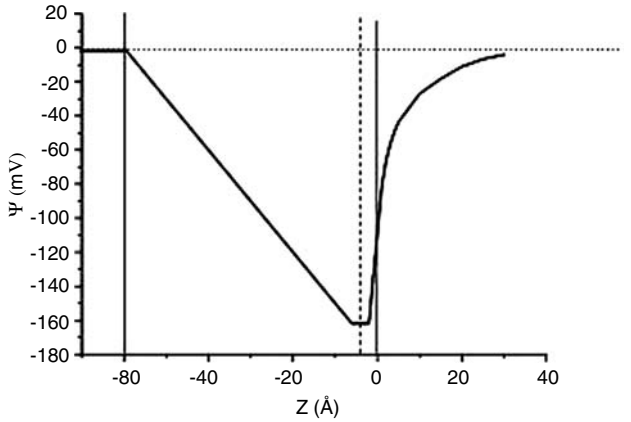

Fig. 1 The model electrostatic potential profile. z (Å) is the position along membrane normal. Two *vertical solid lines* denote the positions of the membrane–solution interfaces (located at $z_w = 0$ and at $z = -60$ Å). The *vertical dashed line* indicate the position of the plane (located at $z_{mc} = z_w - 4$ Å) containing the centers of the charged headgroups

conformations of SDMs were fixed at their solution values. As the result of this, the complete sequence of tBid (residues 60–195 of mouse Bid) was divided into sixsimulation domains (SDM1–SDM6) as shown in Fig. 2. At stage (i), the torsional dihedral angles of residues from these domains were fixed at their NMR solution values, while the dihedrals of interdomain residues (except glycines) were discretized according to their local pattern of available Ramachandran basins. Three types of basins were considered: the extended β-sheet basin, the right-handed α-helical basin and the left-handed α-helix basin. At all we had 3^N different conformations, where N is the number of interdomain residues (without glycines) which were suggested as free to rotate. The glycines within interhelical loops were taken in their NMR conformations at this stage. After that, all these 3^N conformations were undergone to conjugate gradient minimization to eliminate sterically inconsistent ones and only those with free energies differing from that of the lowest energy conformation less than 100 kcal/mol were saved to be further used in simulations as the starting conformations.

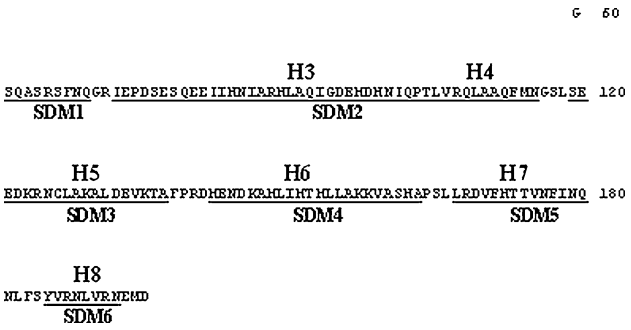

Fig. 2 Simulation domains SDM1–SDM6 (*underlined*) within tBid used at coarse-grained stage (i) of simulations as rigid bodies. α-helices H3 through H8 are *bold-faced*

Furthermore, we followed the Monte Carlo (MC) method in the Metropolis version (Metropolis et al. 1953) in accordance with which each move is accepted if

$$\exp(-\Delta U)/RT) > RN, \tag{11}$$

where RN is the random number uniformly distributed between 0 and 1. Otherwise, the old configuration of the system was counted as the new one.

The generation of sequence of the system configurations for each out of the set of coarse-grained low energy starting structures, selected in accordance with the above described approach, was executing in accordance with the following procedures. First, the generalized coordinates were selected to describe the system dynamics. The position of the protein as a whole relative to fixed coordinate system was described by the coordinates of C_α atom of the first N-terminus peptide unit as well as by three Euler angles (ϕ_{EUL}, Ψ_{EUL}, θ_{EUL}) describing the position of the unit relative to immobile coordinate system. During simulation run for each structure from the set of preliminary selected low energy structures, all dihedral angles for all residues except Gly70 and Gly116 were fixed. Thus, at coarse-grained stage runs (i), each low energy system was described by ten generalized coordinates with six among them describing the position of the protein as a whole and four dihedral angles (φ, Ψ) of rotation about NC_α and $C_\alpha C'$ bonds of Gly70 and Gly116 residues. Every new conformation for each out of the set of coarse-grained conformations of the protein and its new configuration as a whole rigid body were generated by simultaneously subjecting the dihedral angles (φ_i,Ψ_i), of Gly70 and Gly116, as well as Euler angles (ϕ_{EUL} Ψ_{EUL}, θ_{EUL}) and the Cartesian coordinates (X_0, Y_0, Z_0) of the C_α atom of the first N-terminus peptide unit to random perturbations of the type:

$$\Delta\phi_i = \delta\alpha_{max}(2RN_1 - 1), \tag{12}$$

$$\Delta\Psi_i = \delta\alpha_{max}(2RN_2 - 1), \tag{13}$$

$$\Delta X_0 = \delta d_{max}(2RN_3 - 1), \tag{14}$$

$$\Delta Y_0 = \delta d_{max}(2RN_4 - 1), \tag{15}$$

$$\Delta Z_0 = \delta d_{max}(2RN_5 - 1), \tag{16}$$

$$\Delta\varphi_{EUL} = \delta\gamma_{max}(2RN_6 - 1), \tag{17}$$

$$\Delta\Psi_{EUL} = \delta\gamma_{max}(2RN_7 - 1), \tag{18}$$

$$\Delta(\cos\theta_{EUL}) = (\delta\cos\theta_{EUL})_{max}(2RN_8 - 1), \tag{19}$$

where $RN_1 - RN_6$ are random numbers between 0 and 1 and $\delta\alpha_{max}$, δd_{max}, $\delta\gamma_{max}$, $(\delta\cos\theta_{EUL})_{max}$ are maximum variations of the random perturbations of (φ/Ψ) of glycines,

(X_0,Y_0, Z_0), (ϕ_{EUL} Ψ_{EUL}) and cos θ_{EUL}, respectively. The values $\delta\alpha_{max}$ = 3°, δd_{max} = 0.1 Å, $\delta\gamma_{max}$ = 5°, (δcos θ_{EUL})$_{max}$ = 0.073 were chosen. The use of cos(θ_{EUL}) instead of θ_{EUL} allows the generation of Markov chains of configurations by standard Metropolis algorithm (Allen and Tildesley 1987).

At the stage (i), the residues except glycines were represented by alanines, but with electrostatic and hydropathic parameters of polar atoms (if present) from real side chains assigned to alanine C_β atoms. This stage included 100,000 full cycles for each starting structure. After that, the final low energy configurations of protein bound to the membrane not differing by the energy from the lowest energy configuration more than 100 kcal/mol were saved for further refinement at the stage (ii).

Stage (ii)

At this stage, the complete side chains were considered and all dihedral angles were allowed to be varied with the final conformations of backbone and final configurations of the first stage taken as the starting one. This stage included 1,000 Metropolis Monte Carlo cycles for each out of low energy structures selected based on results of the stage (i). At the end, the lowest energy configuration was selected.

To address the convergence problems in the MC search 2–3 independent simulations at stage (i) for each starting structure with different values of starting Euler angles and with different seed numbers of random number generator were realized. The simulations showed that in all instances after 101,000 steps of the two-staged simulations the RMSD of final structures with the correction for translation of tBid as a whole along *X*-, *Y*-coordinate was less than 1.5 Å .

Results and discussions

About 567 structures of tBid were selected at stage (i) by the procedure of coarse-grained ''basin discretization'' of the conformational space with local minimization without the membrane, as described in ''Materials and methods''. These structures with simplified representations of side chains were undergone to 100,000 full cycles MC simulations each with the membrane present and both orientation of the protein and the dihedral angles φ,Ψ of Gly70 and Gly116 within the interhelical loops free to change. With this procedure, the configuration of tBid bound to the membrane and yielding the lowest energy for the solvent–tBid–membrane system together with six other configurations of tBid yielding energies differing from the lowest-energy case by 27, 41, 43, 57, 77, 83 kcal/mol were obtained and saved for further refinement at stage (ii). About 1,000 cycles of the standard Metropolis MC runs with all-atom representation of side chains of tBid and all side-chain and backbone torsional angles free to change were used at stage (ii) to obtain finally the dominant tBid-bound to membrane configuration providing the lowest energy for the solvent–tBid–membrane system.

The structure of membrane–bound tBid

The results of MC simulations are shown in Figs. 3 and 4, in Tables 1, 2 and 3, and Supplementary online data files associated with this article where the data for dominant configuration are listed. Starting from a random, aqueous phase configuration, tBid at its most stable state arranges itself into the configuration bound to the lipid membrane surface without significant insertion of its helices into membrane. With this lowest-energy dominant configuration, the helix H3 is well off the membrane, the helix H4 is shallowly immersed into the membrane with its N-terminus located near the membrane head-group region, the helix H5 is largely exposed to the cytosol with its N-terminus placed near headgroup region of the membrane, the α-helix H6 is shallowly immersed into the membrane by its C-terminal half, while the N-terminal half is exposed to cytosol, the α-

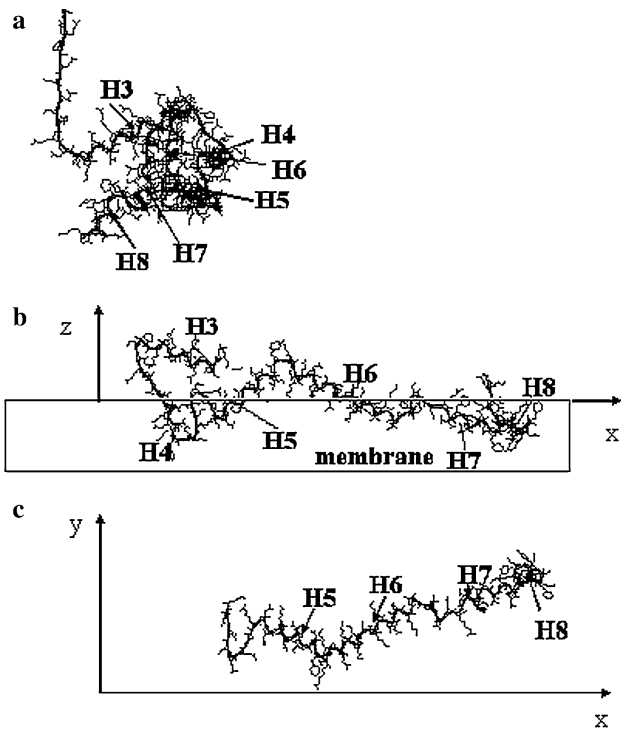

Fig. 3 Results of Monte Carlo simulations of tBid association with the membrane. Starting, solution (**a**), and the membrane-bound (**b**, **c**) states are shown. The projections of tBid bound to membrane on the *X*–*Z* plane (the *z*-axis is perpendicular to the membrane surface) and on the *X*–*Y* plane are represented in **b** and **c**, respectively

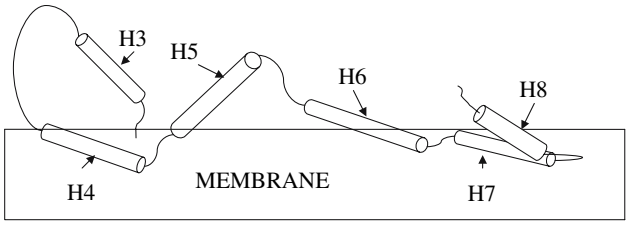

Fig. 4 The schematic diagram of the orientation of tBid helices relative to the membrane. α-helices of tBid are displayed as *cylinders*

helices H7 is shallowly buried into the membrane and H8 is partly buried by its N-terminus half. Five C-terminus residues of tBid as well as the loop between helices H3 and H4 are exposed to cytosol while four N-terminus residues of tBid are buried in the hydrophobic moiety of the membrane slab. Such configuration of tBid, when associated with the membrane, is caused by the balance between the protein electrostatic interactions with the membrane and hydrophobicity. The helices H3, H5 and N-terminus part of H6 are all exposed to the cytosol because of a great number of polar (mostly negatively charged) residues within them. The helices H4 and H7 are shallowly buried owing to their hydrophobic composition, on one hand, and positively charged residues within their N-terminal parts which act as anchors, on the other hand. Two helices H6 and H8 are partly buried due to zwitterionic character of these units with negatively charged residues within the N-terminus part of H6 and C-terminus of H8 and with positively charged residues within the opposite parts of these helices (Fig. 4).

These results are in accordance with the data of Gong et al. (2004) and Mau et al. (2006), which showed that tBid associates with mitochondrial membrane without profound immersion into the lipid membrane. Recently, Oh et al. (2005) with the use of the site-directed spin labeling (SDSL) method of EPR spectroscopy made an effort to localize the helices H3–H8 in greater detail. While taken as a whole, the results of our simulations are in accordance with the data of Oh et al. (2005), which show (i) the presence only of the shallow penetration of tBid into the membrane, (ii) nearly parallel to the membrane surface orientation of helices H6 and H7, (iii) the remote location of helices H3 and H8, (iv) the tilt of the helix H6 to the membrane surface, (v) the localization of H3 helix on the outside of the membrane, (vi) the immersion of the Thr174 of the helix H7 into the membrane, the distinctions in some details take place. Primarily, this concerns the positions of residues Leu149 and Thr152 of H6 and the residue Val190 of H8. In accordance with our simulations, the residues Leu149, Thr152 and Val190 lie near the head-group region of the membrane, while in accordance with the data of Oh et al. (2005), the residues Leu149 and Thr152 of H6 and the residue Val 190 are buried. The reasons of these discrepancies can be of two kinds, one stemming from a coarse-grained character of the simulations and the assumptions made and the other caused by possible artifacts of the experiments. Thus, a further work with the use of more accurate experimental and theoretical approaches is necessary. In every case, the obtained results support the viewpoint (Garcia-Saez et al. 2004; Gong et al. 2004; Oh et al. 2005; Mau et al. 2006) that neither H6, H7, nor the remainder helices of tBid under the association with the mitochondrial membrane are deeply buried enough to penetrate to the other side of the MOM. The present consideration shows that such a behavior of tBid-monomer is caused, apart from intraprotein interactions, by attraction of positively charged side chains of tBid to negatively charged surface, the repulsion of negatively charged, as well as Born solvation energy difference for polar residues in the water and in the lipid membrane. Such a behavior of tBid is analogous to membrane association of the antiapoptopic Bcl-2 family member, Bcl-X_L (Franzin et al. 2004) and is reminiscent of the antimicrobial polypeptides (Epand and Vogel 1999; Vogt et al. 2000; Yamaguchi et al. 2001; Lu et al. 2005), where binding of the polypeptide helices to the bacterial membrane surface is thought to destabilize the membrane and change its morphology, inducing leakage of the cell contents, disruption of the electrical potential and ultimately cell death (Epand and Vogel 1999; Matsuzaki 1999; Zemel et al. 2004).

The conformational rearrangements of tBid upon its association with the membrane

The backbone dihedral angle deviations of tBid associated with the model membrane from starting solution values are shown in Table 3 (the most significant deviations) and in Supplementary data file 2 (the complete listing of the backbone dihedral angles deviations), associated with this article. The results show that the greatest rotations to provide the lowest free energy of the system tBid/membrane/solvent occur within disordered loops between helices H3 and H4, H4 and H5, H5 and H6, H6 and H7, H7 and H8, as well as within the N-terminus loop of the protein preceding the helix H3. Interestingly, that Monte Carlo analysis based on thermodynamics rather than on kinetics results in greatest rotation predominantly about the hinge axes of the residues possessing the smallest side chains. Because the binding of tBid to the MOM is of crucial importance in the apoptosis realization one can conclude that structurally hypervariable regions (SHVRs) within the disordered interhelical loops of tBid are not the passive linkers but may play important roles in apoptosis.

Table 1 Resulting backbone dihedral angles values (φ, Ψ, χ_1) of tBid bound to membrane

	φ_1	Ψ_1	χ_1		φ_1	Ψ_1	χ_1		φ_1	Ψ_1	χ_1
Ser61	103	123	–162	Val106	–63	–27	68	Met151	–68	–39	–173
Gln62	–125	–39	–171	Arg107	–64	–50	–175	Thr152	–72	–31	74
Ala63	–82	71		Gln108	–71	–41	–173	Met153	–73	–31	–165
Ser64	–141	86	–179	Leu109	–56	–50	–177	Leu154	–55	–35	–175
Arg65	–69	90	–165	Ala110	–70	–39		Leu155	–52	–42	–177
Ser66	–158	–47	–179	Ala111	–68	–44		Ala156	–68	–37	
Phe67	–88	95	–174	Gln112	–71	–39	–171	Lys157	–71	–32	–171
Asn68	–117	164	–176	Phe113	–76	–36	–173	Lys158	–72	–39	–171
Gln69	–67	87	–172	Met114	–98	82	–175	Val159	–82	–35	68
Gly70	80	–72		Asn115	–141	124	–178	Ala160	–74	–7	
Arg71	–72	150	–165	Gly116	–98	–50		Ser161	–129	34	–169
Ile72	–128	124	–169	Ser117	–173	104	–175	His162	–62	–36	–178
Glu73	–127	130	–171	Leu118	–147	123	–174	Ala163	–50	–28	
Pro74	–60	143	32	Ser119	–155	150	–167	Pro164	–59	–43	**33**
Asp75	–163	148	–169	Glu120	74	–41	–167	Ser165	–150	16	–171
Ser76	–159	91	–163	Glu121	–107	–158	–174	Leu166	–152	20	–162
Glu77	–81	100	–172	Asp122	–135	78	–175	Leu167	–82	68	156
Ser78	–154	110	–174	Lys123	–80	68	–146	Arg168	–75	–28	–173
Gln79	–141	114	–175	Arg124	–146	153	–163	Asp169	–63	–13	–149
Glu80	–73	147	179	Asn125	–55	–30	–169	Val170	–60	–36	66
Glu81	–130	128	–171	Cys126	–66	–52	–176	Phe171	–79	–38	–178
Ile82	–57	–33	–164	Leu127	–79	–32	–174	His172	–61	–42	173
Ile83	–69	–37	–162	Ala128	–68	–36		Thr173	–59	–11	61
His84	–80	–30	–172	Lys129	–67	–43	174	Thr174	–78	–39	62
Asn85	–72	–43	–174	Ala130	–73	–28		Val175	–67	–32	75
Ile86	–78	–27	–160	Leu131	–66	–20	–174	Asn176	–69	–41	–167
Ala87	–72	–31		Asp132	–85	–49	–166	Phe177	–64	–50	178
Arg88	–74	–43	–176	Glu133	–74	–35	–178	Ile178	–67	–33	–171
His89	–68	–14	–169	Val134	–75	–28	–72	Asn179	–76	–27	–172
Leu90	–76	–27	–173	Lys135	–61	–34	–157	Gln180	–96	25	–169
Ala91	–87	–41		Thr136	–74	–38	57	Asn181	–97	–145	–166
Gln92	–72	–29	–166	Ala137	–87	–32		Leu182	–90	–112	–177
Ile93	–62	–21	–161	Phe138	–123	84	–172	Phe183	–50	–34	–174
Gly94	–57	–36		Pro139	–65	*131*	28	Ser184	–72	–43	–175
Asp95	–85	–44	–162	Arg140	–165	–39	–173	Tyr185	–86	–25	–177
Glu96	–50	–29	–160	Asp141	–116	–52	–180	Val186	–64	–43	65
Met97	–68	–21	–166	Met142	–73	–40	–171	Arg187	–62	–25	–167
Asp98	–52	–38	–165	Glu143	–82	–21	–170	Asn188	–93	–36	–166
His99	–51	–28	–162	Asn144	–74	–48	–175	Leu189	–53	–20	–176
Asn100	–161	62	–167	Asp145	–67	–47	–177	Val190	–61	149	69
Ile101	–145	–170	–156	Lys146	–52	–45	177	Arg191	–70	106	–170
Gln102	–116	82	–170	Ala147	–71	–42		Asn192	–71	83	–162
Pro103	–70	166	33	Met148	–67	–42		Glu193	–70	115	–175
Thr104	–124	132	63	Leu149	–68	–51		Met194	–151	138	–168
Leu105	–96	57	–177	Ile150	–70	–12		Asp195	–91		

Table 2 The distance $(\Delta z)_{a,m}$ (Å) between Cα-atoms of tBid and the membrane

Residues	$(\Delta z)_{a,m}$	Residues	$(\Delta z)_{a,m}$	Residues	$(\Delta z)_{a,m}$	Residues	$(\Delta z)_{a,m}$	Residues	$(\Delta z)_{a,m}$
Ser61	2.61	Arg88(**H3**)	–6.33	Asn115	4.79	Met142(**H6**)	–6.44	Asp169(**H7**)	3.93
Gln62	4.20	His89(**H3**)	–8.40	Gly116	5.91	Glu143(**H6**)	–8.16	Val170(**H7**)	4.17
Ala63	2.75	Leu90(**H3**)	–5.78	Ser117	2.82	Asn144(**H6**)	–9.37	Phe171(**H7**)	1.83
Ser64	–0.55	Ala91(**H3**)	–6.89	Leu118	–0.44	Asp145(**H6**)	–6.02	His172(**H7**)	3.41
Arg65	–1.91	Gln92(**H3**)	–10.52	Ser119	–3.38	Lys146(**H6**)	–4.11	Thr173(**H7**)	6.73
Ser66	–3.56	Ile93(**H3**)	–9.62	Glu120	–7.04	Ala147(**H6**)	–6.59	Thr174(**H7**)	5.53
Phe67	–1.04	Gly94(**H3**)	–8.55	Glu121	–6.18	Met148(**H6**)	–5.87	Val175(**H7**)	3.42
Asn68	0.00	Asp95(**H3**)	–11.98	Asp122	–3.50	Leu149(**H6**)	–2.18	Asn176(**H7**)	6.54
Gln69	2.13	Glu96(**H3**)	–13.85	Lys123	–0.92	Ile150(**H6**)	–2.70	Phe177(**H7**)	8.98
Gly70	–0.78	Met97(**H3**)	–11.40	Arg124	1.46	Met151(**H6**)	–3.86	Ile178(**H7**)	6.28
Arg71	–3.11	Asp98(**H3**)	–12.26	Asn125(**H5**)	2.51	Thr152(**H6**)	–0.65	Asn179(**H7**)	5.09
Ile72	–4.95	His99	–15.35	Cys126(**H5**)	0.74	Met153(**H6**)	1.28	Gln180(**H7**)	8.54
Glu73	–5.31	Asn100	–13.36	Leu127(**H5**)	–2.45	Leu154(**H6**)	–1.54	Asn181	8.37
Pro74	–7.02	Ile101	–9.84	Ala128(**H5**)	–1.60	Leu155(**H6**)	–1.08	Leu182	8.27
Asp75	–5.02	Gln102	–7.49	Lys129(**H5**)	–0.51	Ala156(**H6**)	2.65	Phe183	4.67
Ser76	–6.46	Pro103	–6.51	Ala130(**H5**)	–3.90	Lys157(**H6**)	1.94	Ser184	4.35
Glu77	–4.81	Thr104	–3.49	Leu131(**H5**)	–5.54	Lys158(**H6**)	–0.39	Tyr185(**H8**)	6.71
Ser78	–6.73	Leu105	–2.89	Asp132(**H5**)	–3.67	Val159(**H6**)	2.44	Val186(**H8**)	4.45
Gln79	–6.53	Val106(**H4**)	0.65	Glu133(**H5**)	–4.76	Ala160(**H6**)	5.03	Arg187(**H8**)	1.26
Glu80	–7.45	Arg107(**H4**)	0.77	Val134(**H5**)	–8.30	Ser161(**H6**)	2.60	Asn188(**H8**)	2.26
Glu81	–5.54	Gln108(**H4**)	–0.95	Lys135(**H5**)	–8.21	His162(**H6**)	1.42	Leu189(**H8**)	3.56
Ile82	–6.41	Leu109(**H4**)	1.77	Thr136(**H5**)	–6.52	Ala163	1.57	Val190(**H8**)	0.21
Ile83	–3.10	Ala110(**H4**)	4.38	Ala137(**H5**)	–9.61	Pro164	–1.64	Arg191(**H8**)	–2.13
His84(**H3**)	–3.59	Ala111(**H4**)	3.01	Phe138	–12.18	Ser165	–3.88	Asn192(**H8**)	–3.57
Asn85(**H3**)	–7.11	Gln112(**H4**)	3.47	Pro139	–10.93	Leu166	–1.46	Glu193	–7.17
Ile86(**H3**)	–5.64	Phe113(**H4**)	7.24	Arg140	–12.50	Leu167(**H7**)	0.80	Met194	–9.74
Ala87(**H3**)	–3.45	Met114	7.01	Asp141	–9.69	Arg168(**H7**)	0.27	Asp195	–12.54

Table 3 The backbone dihedral angle deviations ($\Delta\phi$, $\Delta\psi$) between the starting (dihedral angles ϕ_{st}, Ψ_{st}) and final structures. Only great deviations ($|\Delta\phi|/|\Delta\Psi| > 60°$) are shown

Residues	ϕ_{st}	$\Delta\phi$	Ψ_{st}	$\Delta\Psi$	Residues	ϕ_{st}	$\Delta\phi$	Ψ_{st}	$\Delta\Psi$
Gln62	–134.91	10	–66.88	–104	Glu120	62.16	12	29.06	–70
Ser66	–35.92	–122	105.66	–153	Glu121	51.86	–159	67.95	135
Phe67	–177.88	90	93.89	1	Asp122	154.48	71	106.40	–28
Asn68	176.22	121	156.73	7	Arg124	166.72	47	–29.98	–177
Gln69	–175.16	108	73.85	13	Arg140	155.01	40	–169.50	129
Gly70	166.90	–87	133.02	155	Ala163	–116.81	66	81.42	–109
Arg71	–149.39	77	45.12	105	Ser165	–97.19	–53	–12.27	–159
Glu81	66.74	163	115.87	12	Leu167	–51.32	–31	–60.57	129
Ile101	–118.73	–26	72.69	120	Leu182	–94.74	5	75.29	–171
Gln102	157.95	96	55.85	16	Phe183	22.16	–72	–86.62	53
Pro103	–74.96	5	7.16	159	Ser184	–116.01	44	113.50	–157
Thr104	177.58	59	7.59	124	Val190	–57.98	–3	–44.54	–166
Leu105	105.47	159	32.19	–15	Arg191	–59.65	–10	–50.99	–157
Gly116	59.58	–158	154.53	–105	Asn192	–54.98	–14	–48.78	132
Ser117	–85.03	–88	10.47	94	Met194	70.51	168	138.47	0
Leu118	–178.39	31	90.01	96					

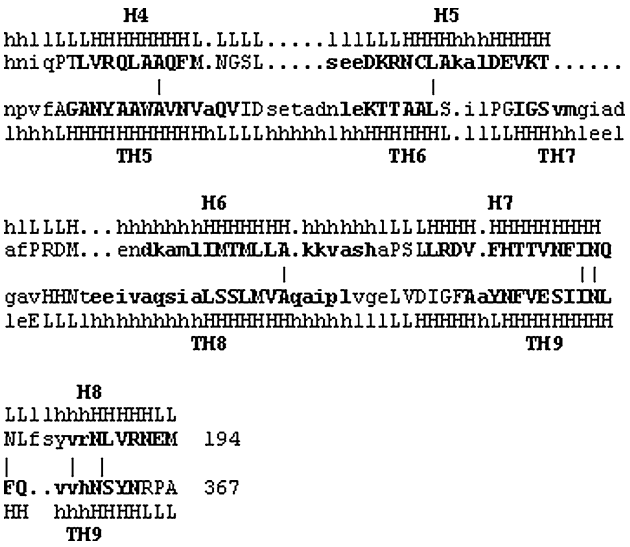

Fig. 5 Structural comparison between tBid (PDB accession number 1ddb) and the diphteria toxin (PDB accession number 1sgk) by DaliLite program Holm and Park 2000. The residues of α-helices are *bold-faced*. H4 through H8 helices of tBid are aligned against TH5–TH9 helices of diphtheria toxin

What are the reasons of the distinction of tBid association with the membrane from that of diphtheria toxin or colicins?

tBid displays structural similarity to transmembrane domains of channel-forming bacterial toxins, such as colicins or diphtheria toxin (Choe et al. 1992; Cramer et al. 1995; Muchmore et al. 1996; Stroud et al. 1998; Zakharov and Cramer 2002; Rosconi et al. 2004). These domains consist of α-helices in which two contiguous α-helices form a helical hairpin structure that is surrounded by other helices. The helical hairpin inserts into the membrane in a transmembrane orientation when the toxin molecules bind to the lipid bilayers. In tBid, helices H6 and H7 correspond to the ''helical hairpin'' regions of these bacterial toxins. Based on this, the insertion of the hairpin formed by helices H6 and H7 into membrane has been suggested (Muchmore et al. 1996; Chou et al. 1999). However, a number of experimental studies (Gong et al. 2004; Oh et al. 2005; Mau et al. 2006) as well as this study show that in the case of tBid the hairpin insertion does not occur. To consider this situation in more detail, the structural comparison between tBid (PDB accession number 1ddb) and the diphtheria toxin (PDB accession number 1sgk) has been undertaken by DaliLite program (Holm and Park 2000) and is shown in Fig. 5. The comparison shows a few essential distinctions between tBid, on the one hand, and the diphtheria toxin and colicin, on the other hand. First, the toxins segments TH8 and TH9 which are homologous to H6 and H7 helices of tBid do not contain charged residues, and, second, the linkers between toxins helices, homologous to H5, H6 and H7 contains the residues with short side chains that makes them as potential candidate hinge groups. Notably, the segments with short side chains are conserved on same positions within the family of bacterial toxins. Taking this into account as well as that the bacterial cell wall membranes are formed by anionic lipids, it is tempting to speculate that the presence both of flexible loops between the helices of hairpin regions and flexible loops edging the hairpin regions, together with lesser bacterial toxins hairpins positive polarity, may be responsible for the insertion of these hairpins into the membrane, unlike tBid hairpin formed by H6 and H7.

Concerted action of pro-apoptopic BAX and tBid to permeabilize MOM

Abundant experimental evidence indicates that tBid must cooperate with multidomain proapoptopic members of Bcl-2 protein family of BAX-type (Desagher et al. 1999; Eskes et al. 2000; Korsemeyer et al. 2000; Wei et al. 2001; Kuwana et al. 2002; Terrones et al. 2004) to kill cells. However, the mechanisms of exactly how tBid functions in concert with BAX or BAX-type proteins are not completely understood at the structural level. One popular model holds that Bid acts via BH3-mediated binding to Bax-type proteins at the MOM followed by their conformational changes, liberation of Bax tail-anchor sequence as well as α5 and α6 helices from sequestration that is necessary for Bax membrane binding and membrane insertion (Letai et al. 2002). On mitochondrial membranes, Bax permeabilizes them either by forming a pore or by modifying an existing pore, resulting in the release of apoptogenic factors, including cytochrome *c* (Antonsson et al. 2000; Belzacq et al. 2003; Annis et al. 2005). Accumulating evidence indicates the possibility of other not necessarily mutually exclusive mechanisms of action in accordance with which tBid cooperates with Bax and cardiolipin to destabilize MOM by monolayer curvature stress and to form non-bilayer lipid structures, such as toroidal lipidic pores or inverted micelles at the MOM (Epand et al. 2002a, b; Basanez et al. 2002; Terrones et al. 2004) analogously to the action of a number of antimicrobial peptides on bacterial cell walls occurring through the mechanism of the lipid membrane destabilization followed by toroidal pore formation (Huang et al. 2004; Huang 2006). By contrast, autonomous pore-forming activity of tBid has been revealed by Schendel et al. (1999), Kudla et al. (2000) and Grinberg et al. (2002). One tempting way to reconcile the observations of autonomous pore-forming behavior of tBid with the seemingly conflicting data of (Gong et al. 2004; Oh et al. 2005; Mau et al. 2006) as well as with our study is through the use of the theory of pep-

tide-induced pore formation in membranes of Huang et al. (2004), whereby the peptide binding to a lipid bilayer causes internal membrane stress (extra-membrane tension) which consequences for the membrane structure largely depend on the molar ratio of the bound—peptide to lipid: if this ratio exceeds some threshold value, the critical structural reorganization of the membrane occurs followed by the pore formation. If to assume that membrane–protein interactions occur in a similar manner, one may expect that some critical number of the proteins should be adsorbed onto the membrane to allow a transmembrane pore to be formed. Thus, one can observe in experiments either pore formation, if the concentration of adsorbed proteins exceeds the pore formation threshold, or the opposite case will take place remaining the membrane in a unpermeabilized state if the number of adsorbed proteins is in under-threshold range.

An alternative plausible explanation for the observation of the membrane insertion of the H6–H7 hairpin is the local fluctuational pH increase in the micro-environment of the H6–H7 hairpin of the membrane-associated tBid and caused by this the deprotonation of positively charged side chains of H6 residues, facilitating the insertion of normally amphipatic H6 segment into the membrane. Once the H6–H7 hairpin is inserted into the membrane, the reverse process, due to a low content of free protons within the lipid phase, becomes unlikely, thus leading to the stabilization of the state with the hairpin inserted into the membrane. Although the proposed hypothesis seems at first glance contrary to the data on Bid and tBid insertion into planar bilayers and liposoms (Schendel et al. 1999) as well as to the data on the insertion of bacterial toxins into biological and model membranes (reviewed in London 1992; Zakharov and Cramer 2002) showing the channel activity of all these proteins at acidic pH and the absence of such an effect at alkaline pH, it can be reconciled with the experimental data mentioned above if to take into account the different character of responses of the proteins to local and whole-cell pH changes. If to assume that the interaction of tBid with the membrane follows the pattern seen with bacterial toxins where the association of the proteins with the membrane is preceded by the attraction of the positively charged proteins for acidic membranes as well as by the formation of intermediate solution conformations of the molten globule type (Lesieur et al. 1997; van der Goot et al. 1991; Bychkova et al. 1996; Chenal et al. 2002; Nam and Choi 2002), one can expect that at high whole-cell pH, due to reduced net charge of tBid (normally +2), both the electrostatic attraction of tBid for the membrane and the formation of the solution intermediates, that is normally stimulated by the protein positive charge, will be suppressed.

Concluding remarks

The obtained results provided insights into the structure of pro-apoptotic protein tBid when it is associated with the model membrane mimicking the MOM. The results show that tBid binds to the membrane formed by negative lipids and that the most stable conformation of tBid monomer bound to the membrane corresponds to the orientation of the most part of the protein near parallel to the membrane surface without significant immersion into the membrane. Thus, association of tBid with the anionic lipidic membrane differs significantly from the binding of the bacterial toxins with the membrane, but bears a significant similarity with the association with the anionic bacterial membranes of antibiotic polypeptides.

The results presented in this paper are obtained with use of the simplistic description of the bilayer by an implicit membrane model. Approaches of this type have been shown in many studies to have the capacity to describe the main thermodynamic and kinetic properties of the peptide–membrane and protein–membrane systems. It should be mentioned that several effects observed during tBid association with the membrane not accounted for by the implicit model are likely to be essential. Among others, the effect of protein-induced bilayer perturbations (membrane stress effect) is of importance for a complete understanding of the protein insertion. Though providing the most realism, the simulations with an explicit representation of the membrane, because of many degrees of freedom involved, require very large amounts of computer time and, therefore, still cannot be applied efficiently even to systems involving medium-size proteins interacting with membranes. As it follows from the current view of the membrane–protein interactions, the protein-induced membrane stress effect is not essential when the membrane-adsorbed, protein to lipid ratio is below some threshold value. Although the exact numerical value of the threshold is not known and cannot be calculated exactly by current theories, the experimental data show that in many cases the association of tBid with the mitochondrial or model membranes occurs without a significant alteration of the membrane tension thus indicating that the concentration of adsorbed proteins is in the under-stress-threshold range. Based on above reasons, it can be suggested that the use of the implicit membrane model and a neglect of the membrane stress are quite justified in these cases both from computational efficiency and physical adequacy standpoints. However, more explicit taking into account of the lipidic phase is necessary in order to describe the interactions of the proteins with membranes when the concentration of the adsorbed proteins reaches the threshold value where protein-induced membrane structural perturbations are of importance.

While the direct experimental data on the structure of tBid associated with the membrane are lacking, the obtained results agree with scanty of low-resolution mainly indirect experimental structural data obtained by glycosylation mapping in a model chimeric system, by measuring the increase of the lipidic monolayer surface pressure, induced by the protein, by use of the EPR site-directed spin labeling method as well as with the use of combination of NMR and CD spectroscopy in model membranes. Though obtained with the use of coarse-grained procedure, the obtained 3D structure is atomistic-resolution data which provide experimentalists with potentially testable hypotheses as to the plausible 3D structure of tBid adsorbed onto the MOM as well as to the orientations of individual structural elements of the membrane-bound tBid relative to the membrane. In addition the data obtained may be used in medicinal structural chemistry in the structure-based drug design.

Acknowledgments The authors thank Prof. Gregory Nikiforovich (Washington University School of Medicine, St Louis, Missouri) for reading the early version of the manuscript and his insightful comments. This work was supported by the Program ''Bioengineering and Biosecurity'' of Republic of Belarus (Grant P-16).

References

Adams JM (2003) Ways of dying: multiple pathways of apoptosis. Genes Dev 172:2481–2495

Allen MP, Tildesley DJ (1987) Computer simulations of liquids. Oxford, Clarendon

Annis MG, Soucie EL, Dlugosz PJ, Cruz-Aguado JC, Penn LZ, Leber B, Andrews DW (2005) Bax forms multispanning monomers that oligomerize to permeabilize membranes during apoptosis. EMBO J 24:2096–2103

Antonsson B, Montessuit S, Lauper S, Eskes R, Martinou JC (2000) Bax oligomerization is required for channel-forming activity in liposomes and to trigger cytochrome c release from mitochondria. Biochem J 345:271–278

Ardail D, Privat J-P, Egret-Charlier M, Levrat C, Lerme F, Louisot P (1990) Mitochondrial contact sites. Lipid composition and dynamics. J Biol Chem 265:18797–18802

Ash WL, Zlomislic MR, Oloo EQ, Tieleman DP (2004) Computer simulations of membrane proteins. Biochim Biophys Acta 1666:158–189

Basanez G, Sharpe JC, Galanis J, Brandt TB, Hardwick JM, Zimmerberg J (2002) Bax-type apoptotic proteins porate pure lipid bilayers through a mechanism sensitive to intrinsic monolayer curvature. J Biol Chem 277:49360–49365

Baumgartner A (1996) Insertion and hairpin formation of membrane proteins: a Monte Carlo study. Biophys J 71:1248–1255

Belzacq AS, Vieira HL, Verrier F, Vandescasteele G, Cohen I, Prevost MC, Larquet E, Pariselli F, Petit PX, Kahn A, Rizzutto R, Brenner C, Kroemer C (2003) Bcl-2 and Bax modulate adenine nucleotides translocase activity. Cancer Res 63:541–546

Benz R, Kottke M, Brdiczka D (1990) The cationically selective state of the mitochondrial outer membrane pore: a study with intact mitochondria and reconstituted mitochondrial porin. Biochim Biophys Acta 1022:311–318

Bond PJ, Sansom MS (2004) The simulation approach to bacterial outer membrane proteins. Mol Membr Biol 21:151–161

Bond PJ, Sansom MS (2006) Insertion and assembly of membrane protein via simulation. J Am Chem Soc 128:2697–2704

Bychkova VE, Dujsekina AE, Klenin SI, Tiktopulo EI, Uversky VN, Ptitsyn OB (1996) Molten globule like state of cytochrome *c* under conditions simulating those near the membrane surface. Biochemistry 35:6058–6063

Chenal A, Savarin P, Nizard P, Guillain F, Gillet D, Forge V (2002) Membrane protein insertion regulated by bringing electrostatic and hydrophobic interactions into play. A case study with the translocation domain of diphtheria toxin. J Biol Chem 277:43425–43432

Choe S, Bennett MJ, Fujii G, Curmi PM, Kantardjieff KA, Collier RJ, Eisenberg D (1992) The crystal structure of diphtheria toxin. Nature 357:216–222

Chou J, Li H, Salvesen G, Yuan J, Wagner G (1999) Solution structure of Bid, an intracellular amplifier of apoptopic signaling. Cell 96:615–624

Chang G, Guida WC, Still WC (1989) An internal coordinate Monte-Carlo method for searching conformational space. J Am Chem Soc 111:4379–4386

Cory S, Huang DC, Adams JM (2003) The Bcl-2 family: roles in cell survival and oncogenesis. Oncogene 22:8590–8607

Cramer WA, Heimann JB, Shendel SL, Deriy BN, Cohen FS, Etkins PA, Stauffacher CV (1995) Structure-function of the channel-forming colicins. Annu Rev Biophys Biomol Struct 24:611–641

Daniel NN, Korsmeyer SJ (2004) Cell death: critical control points. Cell 116:205–219

Desagher S, Osen-Sand A, Nichols A, Eskes R, Montessuit S, Lauper S, Maundrell K, Antonsson B, Martinou JC (1999) Bid-induced conformational change of Bax is responsible for mitochondrial cytochrome c release during apoptosis. J Cell Biol 144:891–901

Ducarme P, Rahman M, Brasseur R (1998) IMPALA: a simple restraint field to simulate the biological membranes in molecular structure studies. Proteins 30:357–371

Dunfield LG, Burgess AW, Scheraga HA (1978) Energy parameters in polypeptides. 8. Empirical potential energy algorithm for the conformational analysis of large molecules. J Phys Chem 82:2609–2616

Efremov RG, Nolde DE, Vergoten G, Arseniev AS (1999a) A solvent model for simulations of peptides in bilayers. I. Membrane-promoting α-helix formation. Biophys J 76:2448–2459

Efremov RG, Nolde DE, Vergoten G, Arseniev AS (1999b) A solvent model for simulations of peptides in bilayers. II. Membrane-spanning α-helices. Biophys J 76:2460–2471

Efremov RG, Volynsky PE, Nolde DE, Dubovskii PV, Arseniev AS (2002) Interaction of cardiotoxins with membranes: a molecular modeling study. Biophys J 83:144–153

Epand RM, Vogel HJ (1999) Diversity of antimicrobial peptides and their mechanisms of ac tion. Biochim Biophys Acta 1462:11–28

Epand RF, Martinou J-C, Fornallaz-Mulhauser M, Hughes DW, Epand RM (2002a) The apoptotic protein tBid promotes leakage by altering membrane curvature. J Biol Chem 277:32632–32639

Epand RF, Martinou J-C, Montessuit S, Epand RM, Yip CM (2002b) Direct evidence for membrane pore formation by the apoptotic protein Bax. Biochem Biophys Res Commun 298:744–749

Eskes R, Desagher S, Antonsson B, Martinou J-C (2000) Bid induces the oligomerization and insertion of BAX into the outer mitochondrial membrane. Mol Cell Biol 20:929–935

Forsten KE, Kosack RE, Lauffenburger DA, Subramanian (1994) Numerical solution of nonlinear Poisson–Boltzmann equation for a membrane electrolyte system. J Phys Chem 98:5580–5586

Fraczkiewicz R, Braun W (1998) Exact and efficient analytical calculation of the accessible surface areas and their gradients for macromolecules. J Comp Chem 19:319–333

Franzin CM, Choi J, Zhai J, Reed D, Marassi FM (2004) Structural studies of apoptosis and ion transport regulatory proteins in membranes. Magn Reson Chem 42:172–179

Garcia-Saez AJ, Mingarro I, Perez-Paya E, Salgado J (2004) Membrane-insertion fragments of Bcl-X_L, Bax, and Bid. Biochemistry 43:10930–10943

Garcia-Saez A, Coraiola M, Dalla Serra M, Mingarro I, Muller P, Salgado J (2006) Peptides corresponding to helices 5 and 6 of BAX can independently form lipid pores. FEBS J 273:971–981

Gong X-M, Choi J, Franzin CM, Zhai D, Reed JC, Marassi FM (2004) Conformation of membrane-associated proapoptopic tBid. J Biol Chem 279:28954–28960

Grinberg M, Sarig R, Zaltsman Y, Frumkin D, Grammatikakis N, Reuveny E, Gross A (2002) tBID homooligomerizes in the mitochondrial membrane to induce apoptosis. J Biol Chem 277:12237–12245

Gross A, McDonnel JM, Korsemeyer SJ (1999a) BCL-2 family members and the mitochondria in apoptosis. Genes Dev 13:1899–1911

Gross A, Yin XM, Wang K, Wei MC, Jockel J, Milliman C, Erdjument-Bromage H, Tempst P, Korsemeyer SJ (1999b) Caspase cleaved BID targets mitochondria and is required for cytochrome c release, while BCL-X_L prevents this release but not tumor necrosis factor R1/FAS death. J Biol Chem 274:1156–1163

Gumbart J, Wang Y, Aksimentiev A, Tajkhotshid E, Schulten K (2005) Molecular dynamics simulations of proteins in lipid bilayers. Curr Opin Struct Biol 15:423–431

Holm L, Park J (2000) DaliLite workbench for protein structure comparison. Bioinformatics 16:566–567

Huang HW, Chen FY, Lee MT (2004) Molecular mechanism of peptide-induced pores in membranes. Phys Rev Lett 92:198304

Huang HW (2006) Molecular mechanism of antimicrobial peptides. The origin of cooperativity. Biochim Biophys Acta 1758:1292–1302

Kessel A, Shental-Bechor D, Haliloglu T, Ben-Tal N (2003) Interaction of hydrophobic peptides with lipid bilayers: Monte Carlo simulations with M2δ. Biophys J 85:3431–3444

Kim TH, Zhao Y, Ding WX, Shin JN, He X, Seo YW, Chen J, Rabinowich H, Amoscato AA, Yin XM (2004) Bid-cardiolipin interaction at Mitochondrial contact site contributes to mitochondrial cristae reorganization and cytochrome c release. Mol Biol Cell 15:3061–3072

Kirkpatrick S, Gelati CD, Vecchi MP (1983) Optimization by simulated annealing. Science 220:671–680

Korsmeyer SJ, Wei MC, Saito M, Weiler S, Oh KJ, Schlesinger PH (2000) Pro-apoptopic cascade activates BID, which oligomerizes BAK or BAX into pores that result in the release of cytochrome c. Cell Death Differ 7:1166–1173

Kudla G, Montessuit S, Eskes R, Berrier C, Martinou JC, Gazi A, Antonsson B (2000) The destabilization of lipid membranes induced by the C-terminal fragment of caspase 8-cleaved bid is inhibited by the N-terminal fragment. J Biol Chem 275:22713–22718

Kuwana T, Mackey MR, Perkins G, Ellisman MH, Latterich M, Schneiter R, Green DR, Newmeyer DD (2002) Bid, Bax, and lipids cooperate to form supramolecular openings in the outer mitochondrial membrane. Cell 111:331–342

Lazaridis T (2005) Implicit solvent simulations of peptide interactions with anionic lipid membranes. Proteins 58:518–527

Lesieur C, Vecsey-Semjen B, Abrami L, Fivaz M, van der Goot FG (1997) Membrane insertion: the strategies of toxins. Mol Membr Biol 14:45–64

Lee J, Scheraga HA, Rackovsky S (1997) New optimization method for conformational energy calculations on polypeptides: conformational space annealing. J Comput Chem 18:1222–1232

Letai A, Bassik MC, Walensky LD, Sorcinelli MD, Weiler S, Korsmeyer SJ (2002) Distinct BH3 domains either sensitize or activate mitochondrial apoptosis, serving as prototype cancer therapeutics. Cancer Cell 2:183–192

Li Z, Scheraga HA (1987) Monte Carlo-minimization approach to the multiple-minima problem in protein folding. Proc Natl Acad Sci USA 84:6611–6615

Li H, Zhu H, Xu CJ, Yuan J (1998) Cleavage of Bid by caspase 8 mediates the mitochondrial damage in the Fas pathway of apoptosis. Cell 94:491–501

London E (1992) Diphtheria toxins: membrane interaction and membrane translocation. Biochim Biophys Acta 1113:25–51

Lu JX, Damodaran K, Blazyk J, Lorigan GA (2005) Solid-state nuclear magnetic resonance relaxation studies of the interaction mechanism of antimicrobial peptides with phospholipid bilayer membranes. Biochemistry 44:10208–10217

Luo X, Budihardjo I, Zou H, Slaughter C, Wang X (1998) Bid, a Bcl-2 interacting protein, mediates cytochrome c release from mitochondria in response to activation of cell surface death receptors. Cell 94:481–490

Lutter M, Fang M, Lun X, Nishijima M, Xie M, Wang X (2000) Cardiolipin provides specificity for targeting of tBid to mitochondria. Nat Cell Biol 2:754–761

Maddox MW, Longo ML (2002) A Monte Carlo study of peptide insertion into lipid bilayers: equilibrium conformations and insertion mechanisms. Biophys J 82:244–263

Matsuzaki K (1999) Why and how are peptide-lipid interactions utilized for self-defense? Magainins and tacheplysins as archetypes. Biochim Biophys Acta 1452:1–10

Mau NV, Kajava AV, Bonfils C, Martinou J-C, Harricane M-C (2006) Interactions of Bax and tBid with lipid monolayers. J Membr Biol 207:1–9

McDonnel J, Fushman D, Milliman C, Korsmeyer S, Cowburn D (1999) Solution structure of the proapoptopic molecule BID: a structural basis for apoptopic agonists and antagonists. Cell 96:625–634

McLaughlin S (1989) The electrostatic properties of membranes. Annu Rev Biophys Biophys Chem 18:113–136

Metropolis N, Rosenbluth AW, Rosenbluth MN, Teller AH, Teller EJ (1953) Equation of state calculations by fast computing machines. J Chem Phys 21:1087–1092

Milik M, Skolnick J (1993) Insertion of peptide chains into lipid membranes: an off-lattice Monte Carlo dynamics model. Proteins 15:10–25

Milik M, Skolnick J (1995) Monte Carlo model of FD and PF1 coat proteins in lipid membranes. Biophys J 69:1382–1386

Muchmore SW, Sattler M, Liang H, Meadows RP, Harian JE, Yoon JE, Nettesheim D, Chang BS, Thompson CB, Wong SL, Ng SL, Fesic SW (1996) X-ray and NMR structure of human Bcl-xL, an inhibitor of programmed cell death. Nature 381:335–341

Mungikar AA, Forciniti D (2004) Conformational changes of peptides at solid/liquid interfaces: a Monte Carlo study. Biomacromolecules 5:2147–2159

Nam GH, Choi KY (2002) Association of human tumor necrosis factor-related apoptosis inducing ligand with membrane upon acidification. Eur J Biochem 269:5280–5287

Nelson AP, Colonomos P, McQuarrie DA (1975) Electrostatic coupling across a membrane with titratable surface groups. J Theor Biol 50:317–325

Némethy G, Pottle MS, Scheraga HA (1983) Energy parameters in polypeptides. 9. Updating of geometrical parameters, nonbonded interactions, and hydrogen bond interactions for the naturally occurring amino acids. J Phys Chem 87:1883–1887

Némethy G, Gibson KD, Palmer KA, Yoon CN, Paterlini G, Zagari A, Rumsey S, Scheraga HA (1992) Energy parameters in polypeptides. 10. Improved geometrical parameters and nonb-

onded interactions for use in ECEPP/3 algorithm with application to proline-containing peptides J Phys Chem 96:6472–6484
Oh KJ, Barbuto S, Meyer N, Kim R-S, Collier RJ, Korsmeyer SJ (2005) Conformational changes in BID, a pro-apoptopic BCL-2 family member, upon membrane binding. J Biol Chem 280:753–767
Opferman JT, Korsmeyer SJ (2003) Apoptosis in the development and maintenance of the immune system. Nat Immunol 4:410–415
Oshima H, Kondo T (1988) Membrane potential and Donnan potential. Biophys Chem 29:277–281
Ozkan SB, Meirovitch H (2004) Conformational search of peptides and proteins: Monte Carlo minimization with an adaptive bias method applied to the heptapeptide deltorphin. J Comput Chem 25:565–572
Peitzsch RM, Eisenberg M, Sharp KA, McLaughlin S (1995) Calculations of the electrostatic potential adjacent to model phospholipid bilayers. Biophys J 68:729–738
Petros AM, Oleiniczak ET, Fesik SW (2004) Structural biology of the Bcl-2 family of proteins. Biochim Biophys Acta 1644:83–94
Pillardy J, Czaplewski C, Wedemeyer WJ, Scheraga HA (2000) Conformation-family Monte Carlo (CFMC): an efficient computational method for identifying the low-energy states of a macromolecule. Helv Chim Acta 83:2214–2230
Pillardy J, Arnautova YA, Czaplewski C, Gibson KD, Scheraga HA (2001) Conformation-family Monte Carlo: a new method for crystal structure prediction. Proc Natl Acad Sci USA 98:12351–12356
Rosconi MP, Zhao G, London E (2004) Analyzing topography of membrane-inserted diphtheria toxin T domain using BODIPY-streptavidin: at low pH, helices 8 and 9 form a transmembrane hairpin but helices 5–7 form stable nonclassical inserted segments on the cis side of the bilayer. Biochemistry 43:9127–9139
Roseman MA (1988) Hydrophobicity of polar amino acid side chains is markedly reduced by flanking peptide bonds. J Mol Biol 200:513–522
Schendel SL, Azimov R, Pawlowski K, Godzik A, Kagan BL, Reed JC (1999) Ion channel activity of the BH3 only BCL-2 family member. BID J Biol Chem 274:21932–21936
Schlame M, Rua D, Greenberg ML (2000) The biosynthesis and functional role of cardiolipin. Prog Lipid Res 39:257–288
Scorrano L, Ashiya M, Buttle K, Weiler S, Oakes SA, Mannela CA, Korsmeyer SJ (2002) A distinct pathway remodels mitochondrial cristae and mobilizes cytochrome c during apoptosis. Dev Cell 2:55–67
Sintes T, Baumgartner A (1998) Membrane-mediated protein attraction. A Monte Carlo study. Physica A 249:571–575
Sperotto MM, May S, Baumgaertner A (2006) Modelling of proteins in membranes. Chem Phys Lipids 141:2–29
Stroud RM, Reiling K, Wiener M, Freymann D (1998) Ion-channel forming colicins. Curr Opin Struct Biol 8:525–533
Sung S-S (1994) Helix folding simulations with various initial conformations. Biophys J 66:1796–1803
Sung S-S (1995) Folding simulations of alanine-based peptides with lysine residues. Biophys J 68:1796–1803
Terrones O, Antonsson B, Yamaguchi H, Wang HG, Liu J, Lee RM, Herrmann A, Basanez G (2004) Lipidic pore formation by the concerted action of proapoptopic BAX and tBid. J Biol Chem 279:30081–30091
Tzlil S, Ben-Schaul A (2005) Flexible charged molecules on mixed fluid lipid membranes: theory and Monte Carlo simulations. Biophys J 88:2391–2402
van der Goot FG, Gonzalez-Manas JM, Lakey JH, Pattus F (1991) A ''molten-globule'' membrane-insertion intermediate of the pore-forming domain of colicin A. Nature 354:408–410
Varfolomeev EE, Ashkenazi A (2004) Tumor necrosis factor: an apoptosis JuNKie? Cell 116:491–497
Vogt B, Ducarme P, Schinzel S, Brasseur R, Bechinger B (2000) The topology of lysine-containing amphipathic peptides in bilayers by circular dichroism, solid-state NMR, and molecular modeling. Biophys J 79:2644–2656
Wang X (2001) The expanding role of mitochondria in apoptosis. Genes Dev 15:2922–2933
Wang K, Yin XM, Chao DT, Milliman CL, Korsmeyer SJ (1996) Bid: a novel BH3 domain-only death agonist. Genes Dev 10:2859–2869
Wei MC, Lindsen T, Mootha VK, Weiler S, Gross A, Ashiya M, Thompson CB, Korsemeyer SJ (2000) tBid, a membrane-targeted death ligand, oligomerizes BAK to release cytochrome *c*. Genes Dev 14:2060–2071
Wei MC, Zong WX, Cheng EH, Lindsten T, Panautsakoupolo V, Ross AJ, Roth KA, McGregor GR, Thompson CB, Korsmayer SJ (2001) Proapoptotic Bax and Bak: a requisite gateway to mitochondrial dysfunction and death. Science 292:727–730
Willis SN, Adams JM (2005) Life in the balance: how BH3-only proteins induce apoptosis. Curr Opin Cell Biol 17:617–625
Winterhalter M, Helfrich W (1992) Bending elasticity of electrically charged bilayers: coupled monolayers, neutral surfaces, and balancing stresses. J Phys Chem 96:327–330
Yamaguchi S, Huster D, Waring A, Lehrer RI, Kearney W, Tack BF, Hong M (2001) Orientation and dynamics of an antimicrobial peptide in the lipid bilayer by solid-state NMR spectroscopy. Biophys J 81:2203–2214
Yin X-M (2006) Bid, a BH3-only multi-functional molecule, is at the cross road of life and death. Gene 369:7–19
Zakharov SD, Cramer WA (2002) Colicin crystal structures: pathways and mechanisms for colicin insertion into membranes. Biochim Biophys Acta 1565:333–346
Zemel A, Ben-Shaul A, May S (2004) Membrane perturbation induced by interfacially adsorbed peptides. Biophys J 86:3607–3619
Zha J, Weiler S, Oh KJ, Wei MC, Korsemeyer SJ (2000) Posttranslational N-Myristoylation of BID as a molecular switch for targeting mitochondria and apoptosis. Science 290:1761–1765
Zhan L, Chen JZY, Liu W-K (2006) Monte Carlo basin paving: an improved global optimization method. Phys Rev E 73:015701 (1–4)